Dynamic Modeling of Reaction Pathways on the Gibbs Energy Surface

ARTICLE *in* INDUSTRIAL & ENGINEERING CHEMISTRY RESEARCH · JANUARY 2000

Impact Factor: 2.59 · DOI: 10.1021/ie9904091

3 AUTHORS, INCLUDING:

Kenneth R. Hall
Texas A&M University
252 PUBLICATIONS **4,052** CITATIONS

Dynamic Modeling of Reaction Pathways on the Gibbs Energy Surface

Srinivas R. Vuddagiri, Kenneth R. Hall, and Philip T. Eubank*

Department of Chemical Engineering, Texas A&M University, College Station, Texas 77843-3122

Based on irreversible thermodynamics and kinetic rate theory developed a number of years ago, modern computer graphics provide new methods to optimize selectivity in multiple reactors or single reactions with multiple reaction mechanisms. Initial conditions and standard Gibbs energies of reaction are sufficient to provide a Gibbs energy surface as a function of reaction extents for the rate-limiting reactions. These conditions also provide the *kinetic boundaries*, as defined here on the extent plane, over which reaction pathways cannot cross. However, product yields higher than those at equilibrium can, nevertheless, be achieved within the kinetic boundaries in some cases. The industrial term for this feat, *cheating thermodynamics*, is shown to be incorrect. For simplicity the results presented are for perfect gas mixtures under isobaric/isothermal reaction conditions; other cases are cited. Last, electrical analogue diagrams for complex reaction systems and the meaning of the term *rate limiting* are considered.

Introduction

Technical personnel of chemical companies sometime disclose that they have *cheated thermodynamics* in producing a higher yield of the desired product than that given by thermodynamic equilibrium. While this is clearly impossible starting only with reactants of a truly single elementary reaction operating at fixed pressure and temperature, it is possible when more than one reaction is involved including the common case where an apparent single reaction is actually composed of a combination of mechanistic reactions, often involving radicals. Because higher yields mean higher profits, it is important to examine reaction pathways on the nonequilibrium Gibbs surface to optimize selectivity by use of various catalysts and/or variations of pressure and temperature during the reaction. For isothermal/isobaric pathways, the natural energy function is the Gibbs energy, G, whose total value must decrease with time in conjunction with the second law of thermodynamics.

A new method to optimize chemical processes is discussed in this paper with the goal to answer such fundamental questions. The main idea behind this method is to model kinetic pathways directly on thermodynamic surfaces. This method can be used for chemical systems that end very far from or very close to the global equilibrium.

Denbigh[1] notes that one of the few truly elementary reactions is the formation and decomposition of HI. Because each net or apparent reaction is actually composed of a number of elementary, mechanistic reactions, this paper addresses virtually all reacting systems.

Literature: The Fundamentals

The interaction between irreversible thermodynamics and kinetic rate theory is now better understood, at least from a theoretical viewpoint.[2] Engineering applications involving multiple reactions are numerous. A fundamental understanding of the kinetics and nonequilibrium thermodynamics underlying this subject was gained from 1945 to 1980 with contributions from prominent kineticists (e.g., Boudart) and thermodynamicists (e.g., Prigogine). This literature linking irreversible thermodynamics and kinetics rate theory was primarily concerned with answering two questions. The first question was, what restrictions are imposed upon the form of the forward, reverse, and net rate by conditions that hold at equilibrium? The second question concerns the relationship between the ratio of forward to reverse rate constants to the equilibrium constant (K_e).[3−7] It had been shown that the rate of a chemical reaction close to equilibrium is directly proportional to the free energy difference between reactants and products by de Donder[8] on the basis of his affinity function, Prigogine[9] on the basis of the Chapman−Enskog model, Manes et al.[10] using purely mathematical models, and Gilkerson et al.,[11] Hollingsworth,[12] Zwolinski and Marcus[13] and Van Rysselberghe[14] using kinetic rate theory. This relation can be shown using rate theory and making simplifying approximations at equilibrium. The ratio of forward rate ($\vec{r}$) to reverse rate ($\overleftarrow{r}$) for an elementary reversible reaction can be written as

$$(\vec{r}/\overleftarrow{r}) = \exp(-\Delta G/RT] \tag{1}$$

where ΔG is an instantaneous Gibbs energy change upon reaction, T is the system temperature, and R is the gas constant. Here

$$\Delta G_j \equiv \sum_i \nu_{ij}\hat{\mu}_i \equiv -\mathcal{A}_j \tag{2}$$

where ν_{ij} is the stoichiometric coefficient of component i for reaction j, $\hat{\mu}_i$ is the chemical potential of component i, and $\mathcal{A}_j$ is the affinity for reaction j. While it has been recently[15] well argued that affinities should be used because of their relation to reaction entropy production as

* To whom all correspondence should be addressed. Tel.: (409) 845-3339. Fax: (409) 845-6446. E-mail: p-eubank@tamu.edu.

10.1021/ie9904091 CCC: $19.00
Published on Web 01/22/2000

$$(dS_R/dt) = \sum_j (\mathcal{A}_j/T)(d\xi_j/dt) \geq 0 \quad (3)$$

the choice between ΔG and $\mathcal{A}$ remains that of sign and is arbitrary.

Near equilibrium, where $|\Delta G/RT| \ll 1$, eq 1 can be expanded using the exponential series

$$(\vec{r}/\bar{r}) = \sum_{n=0}^{\infty} [(-\Delta G/RT)^n/n!] = 1 - \Delta G/RT + (\Delta G/RT)^2/2 - (\Delta G/RT)^3/6 + \text{higher degree} \quad (4)$$

When second degree and higher terms are neglected, eq 4 simplifies to

$$(\vec{r}/\bar{r}) = 1 - \Delta G/RT \quad (5)$$

Prigogine et al.[9] from experiment and Manes et al.[10] from their physical observations substantiated this result. While often ignored in textbooks, it is important to keep in mind that when a single elementary reaction is well removed from equilibrium, use of eq 5 in place of eq 1 results in errors of 4.9, 14.2, and 22.9% when the instantaneous, dimensionless Gibbs energy of reaction is -0.1, -0.3, and -0.5, respectively.

When the net or apparent reaction is not elementary but rather composed of a number of elementary, mechanistic reactions, we follow Boudart,[7] who summarized much of the previously mentioned literature of 1945–1980. The forward to backward rates of the net reaction were shown to be

$$(\vec{r}/\bar{r}) = \exp[\sum_{j=1}^{\mathcal{R}} (-\Delta G_j/RT] \quad (6)$$

where $\mathcal{R}$ is the total number of independent, mechanistic reactions. Equation 6 reduces to eq 1 for a single, elementary reaction. The average stoichiometric number $\bar{\chi}$ of the net reaction was defined by Temkin[16] to be

$$\bar{\chi} \equiv \{[\sum_{j=1}^{\mathcal{R}} (-\Delta G_j)\chi_j/RT]/\sum_{j=1}^{\mathcal{R}} (-\Delta G_j/RT)\} = (-\Delta G/RT)/\sum_{j=1}^{\mathcal{R}} (-\Delta G_j/RT) \quad (7)$$

where $-\Delta G/RT$ is for the net reaction.

For example, in the Haber process for producing ammonia using nitrogen gas and hydrogen gas over a catalyst, the overall reaction is given by

$$N_2 + 3H_2 = 2NH_3 \quad (8)$$

The overall reaction can be broken down into five elementary mechanistic steps with their stoichiometric values (χ_j) as related to the overall reaction given in square brackets:

$$N_2 \rightarrow 2N \quad [1] \quad (9a)$$

$$H_2 \rightarrow 2H \quad [3] \quad (9b)$$

$$N_2 + H \rightarrow NH \quad [2] \quad (9c)$$

$$NH + H \rightarrow NH_2 \quad [2] \quad (9d)$$

$$NH + H \rightarrow NH_3 \quad [2] \quad (9e)$$

The sum of the mechanistic steps times the value given in the brackets, [ ], is equal to eq 8. In other words, with these stoichiometric values there will be no accumulation of any of the intermediates: N, H, NH_2, and NH. For example, if the reaction $H_2 \rightarrow 2H$ is slow and the other four reactions instantaneous, then $\bar{\chi} = \chi_b = 3$. However, the rate-limiting reaction is usually the fourth reaction so that $\bar{\chi}$ is near 2.

Continuing the general analysis, the familiar thermodynamic relations for the jth reaction and for the net reaction

$$\Delta G/RT = \Delta G^{\ominus}/RT + \ln K; \quad \Delta G^{\ominus}/RT = -\ln K_e, \quad \text{where } K \equiv \prod_i a_i^{\nu_i} \quad (10)$$

a_i is the activity of component or species i, $\Delta G^{\ominus}/RT$ is the standard Gibbs energy of reaction j or of the net reaction, and K_e is the equilibrium constant for that reaction, are substituted into eq 6 to provide for the net reaction:

$$(\vec{r}/\bar{r}) = (K_e^{1/\bar{\chi}})K^{-1/\bar{\chi}} \quad (11)$$

Boudart[7] proved that when the kinetic rate expressions are written in the form

$$(\vec{r}/\bar{r}) = (\vec{k}/\bar{k})\prod_i (a_i)^{\bar{\alpha}_i - \bar{\alpha}_i} \quad (12)$$

where $\vec{k}$ is the forward rate constant of the net reaction, $\bar{k}$ is its backward rate constant, and α_i is the order of the net reaction for component i in the forward and backward directions, the leading constant multipliers of eqs 11 and 12 are equal or

$$(\vec{k}/\bar{k}) = K_e^{1/\bar{\chi}} \quad (13)$$

We further note the equality of the remaining terms on the right-hand side of eqs 11 and 12, both involving dynamic activities of the various species along the reaction pathway:

$$\vec{\alpha}_i - \bar{\alpha}_i = -\nu_i/\bar{\chi} \quad (14)$$

Equation 14 carries the usual sign convention that reaction products have positive stoichiometric coefficients whereas reactants have negative coefficients. For our net reaction, the order of the forward reaction would normally be zero for products as would the order of the backward reaction for reactants, unless the same component appears as both a reactant and a product. Thus, eq 14 normally simplifies to $\vec{\alpha}_i = -\nu_i/\bar{\chi}$ for reactants and $\bar{\alpha}_i = \nu_i/\bar{\chi}$ for products.

Equation 14 provides a major reason why kinetic order and stoichiometric coefficients are often not the same. Indeed, kinetic rate data can be used to find $\bar{\chi}$ and thus χ_j when there is only one rate-limiting mechanistic reaction providing consistency or inconsistency with a set of proposed elementary, mechanistic equations. This exercise provides only necessary but not sufficient conditions for the correctness of the proposed mechanistic equations. One can also appreciate why α_i is not restricted to an integer or reciprocal of an integer and why it may vary with temperature and pressure.

Finally, we continue the general analysis to relate rate expressions to Ohm's law to connect with the Electrical Analogues section. When eqs 10–14 are used

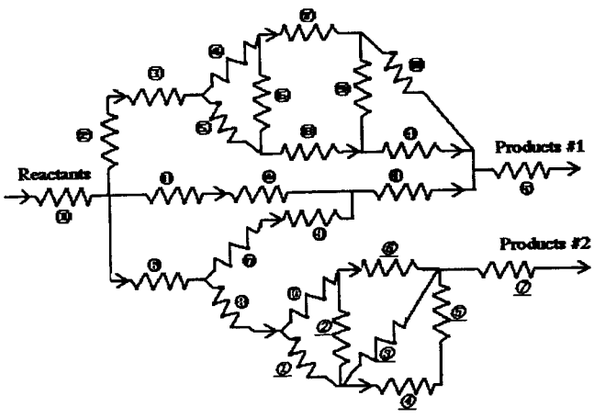

Figure 1. Complex network of 27 chemical reactions as represented by an electrical resistance diagram.

to solve for the overall reaction rate r of the net reaction, $\vec{r} - \overleftarrow{r}$,

$$r = \vec{k}[1 - (K/K_e)^{1/\bar{\nu}}]\prod_i (a_i)^{\bar{\alpha}_i} \qquad (15)$$

In simple analogy to Ohm's law, $\vec{k} \propto (\text{resistance})^{-1}$ and $[1 - (K/K_e)^{1/\bar{\nu}}]\prod_i (a_i)^{\bar{\alpha}_i}$ can be considered the thermodynamic potential $\mathscr{P}$ for the net reaction, similar to the definition of Happel.[17]

Electrical Analogues

Rate expressions for complex chemical reactions can be viewed from electrical resistance diagrams with reactions in series (consecutive), parallel (simultaneous/competing/*side*), delta (triangular), and Y-junctioned.[18] As noted above, a single reaction may also be the result of adding a number of mechanistic equations, often involving radicals, to provide the single apparent reaction. Figure 1 illustrates a complex set of 27 reactions, similar to a real case involved with the production of a new medical drug. The valued final product could be one of the compounds labeled in Products #1 or in Products #2 or both. Instantaneous reactions (no resistance) can be eliminated from the network and the rate-limiting reactions identified. Some branches of the network are effectively blocked by very slow reactions (very high resistance) so the original network can often be simplified to one or two open channels each containing one or two intermediate rate-limiting reactions.

While some believe that electrical diagrams cannot capture the complexity of multiple chemical reactions, it appears to us that only some alterations are needed. First, to capture the dynamics or time dependency of reactions, capacitors must be added in parallel with each resistor to provide inertial or storage ability. Figure 2 illustrates this addition for the simple series reaction A (▲) + 2B (●) = C (■) + B = D (◆). Forget about electrons and imagine that there are originally four positive charges (one ▲ and three ●) on the left plate of capacitor C_1. At zero time we close both switches; in going through resistor R_1 each molecule of A takes two molecules of B to make a molecule of C. If the first reactions are fast, we soon have two positive charges (one ● and one ■) on the left plate of capacitor C_2, as shown in Figure 2. If the second reaction is also fast, we will soon have one positive charge (◆) to the right of resistor R_2. We can also see the well-known maximization of moles of C when both reactions are slow as quantified in terms of the charge (■) on the left plate of capacitor C_2. When a reaction is unidirectionally forward, we show in a forthcoming paper that $\vec{k} = (RC)^{-1}$ for eq 15.

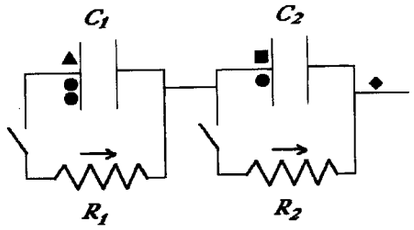

Figure 2. Complete electrical diagram for the reaction A (▲) + 2B (●) = C (■) + B = D (◆), where the first reaction is represented by a resistor R_1 in parallel with a capacitor C_1 and the second reaction by R_2 in parallel with C_2. The two reactions are themselves in series (consecutive). Such a resistor/capacitor pair should thus replace each resistor of Figure 1. One ▲ and two ● positive charges are shown on the left plate of capacitor C_1 representing the initial condition before the two circuit switches are closed. One ● and one ■ charges are shown on the left plate of capacitor C_2 representing conditions at a later time whereas one ◆ charge is shown to the right of resistor R_2 representing a much later time. This simple scenario would be correct only if the first reaction is much faster than the second (kinetics) and if both $(\Delta G°/RT)_1$ and $(\Delta G°/RT)_2$ are strongly negative, causing both reactions to drive to the right (thermodynamics).

While the basic dynamics of the system has been captured, we have taken considerable license with electrical circuitry including distinguishable symbolic charges and violation of charge conservation. While others can no doubt improve on this crude analogy, our main point is that electrical diagrams can be invaluable aids when dealing with complex reaction systems as shown in Figure 1. Following the equations of the previous section, this electrical analogy can be applied regardless of the kinetic order of a particular reaction; for example, the first reaction may be second order while the second reaction is first order. In the special case where all of the elementary reactions are first order, the differential rate equations can be easily combined as shown by Wei and Prater.[19,20] Interestingly, these authors used a hydrodynamical analogy for a triangular reaction.

Rate-Limiting Reactions

The kinetic concept of *rate limiting*, perhaps better termed *rate determining*,[21] is best understood with resistance diagrams.[1] In the case of a simple series circuit like Figure 2, we have different potentials across the two resistors as well as different rates of electrical current. If resistor 1 has a much higher resistance as compared to resistor 2, then resistor 1 is commonly termed rate limiting. However, if the two resistors were placed in a simple parallel circuit, then which would be rate limiting? Here the potential is the same across the two resistors and the total current is proportional to $[R_1^{-1} + R_2^{-1}]$ so a 10% change in R_2 has a greater effect on the total current than does a 10% change in R_1. Here R_2 is definitely rate determining. Of course, the two reactions (two resistors) are generally making different products so we must also ask *the rate of making what*? Then the reactor making what we want is rate limiting. Reflecting back on the series case of Figure 2, if chemical C is the desired product rather than D, then we hope the first reaction is fast and the second slow; we would

likely then term the first reaction as rate limiting regardless of the magnitude of the two resistances. This designation would be reversed if we started with only D as a reactant. Thus, both initial conditions, what product we seek, and the configuration of the electrical network are all important in defining what is meant by rate limiting.

It is perhaps easier to define what rate limiting is not and that is it is not thermodynamic. The fundamental equation of chemical reaction equilibria contained in eq 10

$$(\Delta G^{\ominus}/RT)_j = -\ln K_{e,j} \tag{16}$$

applies only at equilibrium for reaction j as a result of setting $(\Delta G/RT)_j$ equal to zero. Note that $(\Delta G/RT)_j$ is very different from $(\Delta G^{\ominus}/RT)_j$. The latter is purely a thermodynamic property which varies only with temperature, how the reaction j equation has been written, and the standard states selected for each component involved in reaction j. It assumes that we start with ν_{ij} moles of the reactants in their respective standard states and that we have a complete reaction to provide ν_{ij} moles of the products also in their respective standard states.[22] It is further time independent and eventually determines global equilibria. Its only connection with kinetics is that by eqs 13 and 16

$$(\vec{k}/\overleftarrow{k})_j = [\exp(-\Delta G^{\ominus}/RT)_j]^{1/\chi_j} \tag{17}$$

where the forward and backward kinetic rate constants are those at the time and conditions corresponding to equilibria for net reaction j. While these values may not change greatly along a reaction pathway at constant temperature and pressure with fixed catalysis, it is important to understand that the value of $(\Delta G^{\ominus}/RT)_j$ does not set the reaction rate constants. They may both be very large values or both very small and still have the same ratio. The notion that one can determine which reactions are slow, and thus rate limiting, by examination of which $(\Delta G^{\ominus}/RT)_j$ is the least negative is false.

Equations: Definition of G^*

We return to the simple series reaction A + 2B = C + B = D considered as two elementary reactions, with the net reaction being A + 2B = D. With χ set to unity for both the elementary reactions and the net reaction, repeated application of eq 15 provides

$$r_1 = \left(\frac{d\xi_1}{dt}\right) = \vec{k}_1[1 - (K_1/K_{e,1})]a_A a_B = \vec{k}_1\mathscr{P}_1$$

$$r_2 = \left(\frac{d\xi_2}{dt}\right) = \vec{k}_2[1 - (K_2/K_{e,2})]a_B a_C = \vec{k}_2\mathscr{P}_2 \tag{18}$$

$$r_n = \left(\frac{d\xi_n}{dt}\right) = \vec{k}_n[1 - (K_n/K_{e,n})]a_A a_B{}^2 = \vec{k}_n\mathscr{P}_n$$

where the subscript n denotes the net reaction and $\mathscr{P}_j$ is the potential for reaction j for use in Ohm's law as outlined in the previous section Electrical Analogues. Using both the Arrenhius equation and the second law of thermodynamics, $K_{e,j}$ can be written as

$$K_{e,j} = \exp[\Delta H_j^{\ominus}/RT - \Delta S_j^{\ominus}/R] = (\vec{k}_j^*/\overleftarrow{k}_j^*)\exp[\vec{E}_{A,j}/RT - \overleftarrow{E}_{A,j}/RT] \tag{19}$$

where $\vec{k}_j^*$ and $\overleftarrow{k}_j^*$ are the preexponential factors for the forward and reverse rate constants, respectively; $\Delta H_j^{\ominus}/RT$ and $\Delta S_j^{\ominus}/RT$ are the standard enthalpy and entropy changes; and, finally, $\vec{E}_{A,j}$ and $\overleftarrow{E}_{A,j}$ are the forward and reverse activation energies, respectively, for reaction j. All of the terms in eq 19 vary only with temperature, whereas the potential $\mathscr{P}_j$ involves the equilibrium constant as well as the instantaneous activities of the various species along the reaction pathway.

From the mass balance side, we use extents ξ_j (reaction coordinates) in the usual fashion[27] to bring starting conditions into the equations:

$$\sum_j \nu_{ij}\xi_j \equiv (n_i - n_i^0) \tag{20}$$

where n_i is moles of component i, n_i^0 is initial moles of i, n_T^0 is the total initial moles, and ν_j is the net stoichiometric coefficient of reaction j or $\nu_j = \sum_{i=1}^{\mathscr{N}}\nu_{ij}$, where the total components $\mathscr{N}$ includes all species including radicals and intermediates.

The total Gibbs energy for a reacting system can be written, in general, as

$$G_T = \sum_{i=1}^{\mathscr{N}} n_i\hat{\mu}_i = \sum_{i=1}^{\mathscr{N}}[n_i^0 + \sum_{j=1}^{\mathscr{R}}\xi_j\nu_{ij}][\hat{\mu}_i^{\ominus} + RT\ln a_i] \tag{21}$$

where $\hat{\mu}_i^{\ominus}$ represents the standard state of component i, which except for the *aqueous* standard state is for pure component i, $\hat{\mu}_i^{\ominus} = \mu_i^{\ominus}$, where the common standard states are gas, liquid, and solid, with the gas being a pure, perfect gas at temperature T and a pressure of 1 bar. While that is the standard state used here for all components, different standard states can be used for the various components as long as they are used *consistently* throughout the calculations. This is due to the fact that the activity is itself biased to a selected standard state, $a_i = \hat{f}_i/\hat{f}_i^{\ominus}$, so that the last bracket of eq 21 requires only that the same standard state be used for the fugacity $\hat{f}_i^{\ominus}$ as that used for the chemical potential $\hat{\mu}_i^{\ominus}$ for each separate component i. For the gas standard state, this fugacity is the reference pressure of $P^{\ominus} = 1$ bar.

After some algebra, eq 21 can be written as

$$\left[\frac{G_T - \sum_i n_i^0\hat{\mu}_i^{\ominus}}{n_T^0 RT}\right] \equiv G^* = \sum_j\left(\frac{\xi_j}{n_T^0}\right)\left(\frac{\Delta G_j^{\ominus}}{RT}\right) + \sum_i\left(\frac{n_i}{n_T^0}\right)\ln a_i \tag{22}$$

which is valid under the general conditions of multiple phases whenever dynamic phase equilibrium may be assumed along the reaction pathway. This is because the activity or chemical potential is the same for species i in each phase even though we are not at chemical equilibrium. The moles of i are merely replaced by the sum of moles of i in the vapor phase plus moles of i in the liquid phase, etc. Equation 20 allows n_i to be replaced by the extents. Under the phase equilibrium assumption, activities may be evaluated from the most convenient phase with care that the selected phase does not disappear along the reaction pathway. Note that the minimization of G^* is the same as the minimization of

G_T as the two differ by a constant that does not change along the reaction pathway.

For simplicity, we here assume gas-phase reactions with the additional assumption of perfect (ideal) gas mixtures. Under these assumptions, the activities become partial pressures, $p_i \equiv Py_i$, where y_i is the mole fraction of component i.

$$y_i = [(n_i^0 + \sum_{j=1}^{\mathscr{R}} \nu_{ij}\xi_j)/(n_T^0 + \sum_{j=1}^{\mathscr{R}} \nu_j\xi_j)] \tag{23}$$

Equation 22 simplifies to

$$\left[\frac{G_T - \sum_i n_i^0 \mu_i^\ominus}{n_T^0 RT}\right] \equiv G^* = \sum_j \left(\frac{\xi_j}{n_T^0}\right)\left(\frac{\Delta G_j^\ominus}{RT}\right) + \sum_i \left(\frac{n_i}{n_T^0}\right) \ln\left(\frac{Py_i}{P^0}\right) \tag{24}$$

where eqs 20 and 23 can be used to replace n_i and y_i, respectively, with the extents. For analysis of the graphs and results to follow, it is important to note that the right-hand side of the above equation can be written in terms of starting moles, extents, pressure, and the dimensionless, standard Gibbs energy changes. Thus, the graphs of the next section are of the form

$$G^* = G^*[\xi_j, n_i^0, \Delta G_j^\ominus/RT] \tag{25}$$

Graphical Results

In the course of multiple reactions occurring with time at constant temperature and pressure, the total Gibbs energy must decrease. To track the pathway of such reactions, it is advantageous to plot the Gibbs energy as a function of the extent ξ_j of the $\mathscr{R}$ independent reactions. Actually, we need only plot G^* versus the extents of the reactions that are rate determining. It is not necessary to plot the extent of *fast-assumed instantaneous* reactions as their extents can be found independently by using their local equilibrium equations.

We demonstrate these results with the simple series reaction used previously: A + 2B = C + B = D. Being a series reaction, the rate-determining reactions are the slow ($\mathscr{J}$) ones as opposed to the fast ($\mathscr{F}$) ones. If there were more than two independent reactions in series that were slow, then the graphs would be into the hyperspace. We further assume isothermal/isobaric conditions with a perfect gas mixture. A number of interesting results are found even with all of these simplifying assumptions and, indeed, the assumptions make an understanding of the results far easier.

In eq 25, we specify the starting conditions, n_i^0, and the standard Gibbs energies of reaction, $\Delta G_j^\ominus/RT$, leaving $G^*[\xi_1,\xi_2]$ for the graphs. Two types of graphs are presented. The first type is a *3D computer graphic* generated from standard Apple Computer software. This graph provides the viewer with an overview of (1) where the reactions are starting, the initial conditions, (2) the global equilibrium position, and (3) the Gibbs surface available for various reaction pathways. Figure 3 is an example of such a 3D graph where $\Delta G_1^\ominus/RT = -1$, $\Delta G_2^\ominus/RT = -1$, $n_A^0 = 1$, and $n_B^0 = 2$. While the system pressure in eq 24 has been set to 1 bar, the temperature need not be defined but does correspond in practice to a temperature where the standard Gibbs energy of reaction (taken at that temperature) of the first reaction when divided by RT is -1 and likewise is -1 for the second reaction. Figure 3 also presents the idea that, at a given time t corresponding to a point on the Gibbs surface, the rate-constant vector $\vec{k}$, composed of components $\vec{k}_1$ and $\vec{k}_2$ in eq 18, provides the direction of the reaction in the next time increment dt when the extents change by dξ_1 and dξ_2, respectively. This idea is not exactly correct as the direction of the pathway vector is dξ_2 / d$\xi_1 = (\vec{k}_2/\vec{k}_1)(\mathscr{P}_2/\mathscr{P}_1)$, by eq 18, so the thermodynamic potentials $\mathscr{P}_j$ are also involved. Nevertheless, it is useful to think of irreversible thermodynamics as supplying the Gibbs surface and kinetics the instantaneous direction on the surface. Figure 3 has an arbitrary constant of 3 added to G^* to improve the graphics.

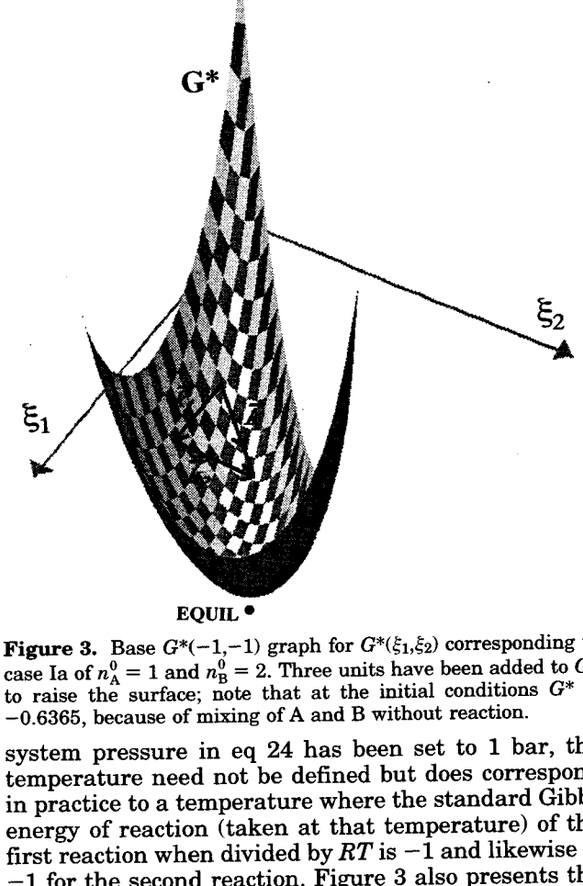

Figure 3. Base $G^*(-1,-1)$ graph for $G^*(\xi_1,\xi_2)$ corresponding to case Ia of $n_A^0 = 1$ and $n_B^0 = 2$. Three units have been added to G^* to raise the surface; note that at the initial conditions G^* is -0.6365, because of mixing of A and B without reaction.

The second type of graph is a *2D contour map*, familiar to mountain hikers as a topographical map. Elevation is replaced by G^*, and the two extents pinpoint the planar surface location as shown by Figure 4, which has conditions identical with those of Figure 3. The true value of G^* at the global equilibrium is -1.1689 from eq 24 at $\xi_1 = 0.73$ and $\xi_2 = 0.39$. The *kinetic boundaries* are shown in Figure 4. If the first reaction is instantaneous ($\mathscr{F}$) and the second slow ($\mathscr{J}$), the pathway starts from [0, 0] for $[\xi_1,\xi_2]$ and jumps to [0.61, 0] where the true $G^* = -0.9678$; it should be kept in mind that ideal solution mixing of 1 mole of A with 2 mol of B at coordinate [0, 0] lowers G^* from zero to -0.6365, as noted in Figure 3. Our ($\mathscr{F}/\mathscr{J}$) case at [0.61, 0] then moves to the interior of the triangle of Figure 4 as the slow second reaction begins to occur. It proceeds upward and to the right along the line marked F until reaching the global equilibrium. Conversely, if the first reaction is slow and the second instantaneous ($\mathscr{J}/\mathscr{F}$),

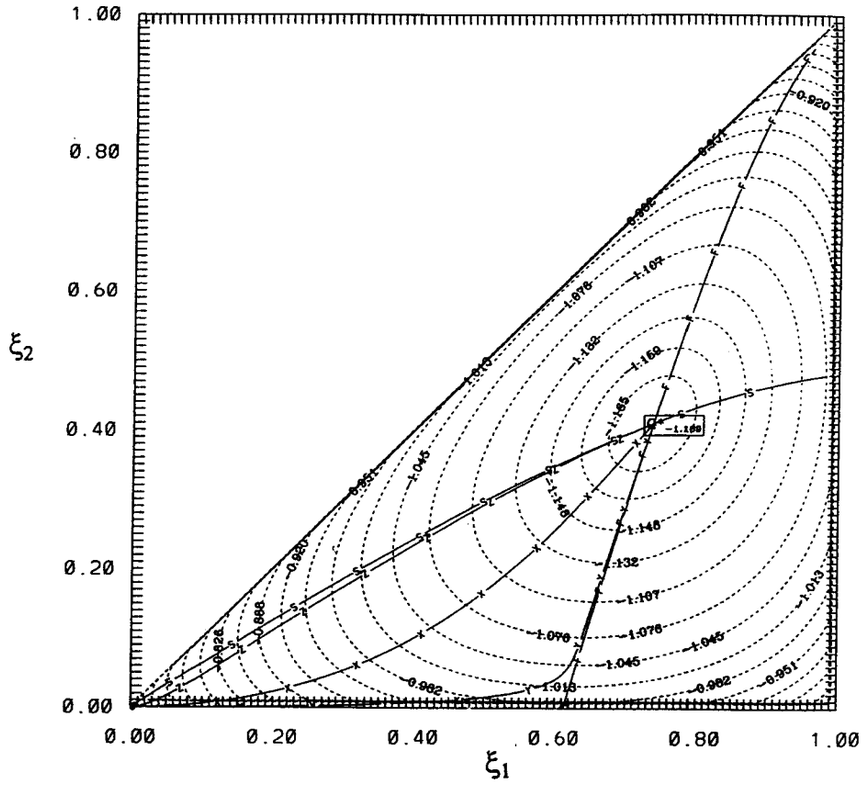

Figure 4. Gibbs energy contour diagram for $G^*\{(\xi_1,\xi_2), (n_A^0 = 1, n_B^0 = 2), [(\Delta G^\ominus/RT)_1 = -1, (\Delta G^\ominus/RT)_2 = -1]\}$ for the reaction A + 2B = 1 = B + C = 2 = D; Series Case; the pathways X, Y, and Z correspond to k_2/k_1 being unity, 20.09, and 0.049 79, respectively.

the pathway starts again from the origin of Figure 4 but moves upward and to the right along the line marked S until reaching the global equilibrium. The lines F and S form what we define as the *kinetic boundary*. When the initial conditions and standard Gibbs energies have been fixed, no reaction pathway can cross this boundary because the result would be one or more negative kinetic rate constants k_j. Both the starting point and the global equilibrium point lie on apexes of the kinetic boundary; the extension of the curves F and S beyond the global equilibrium point and into the upper right section of Figure 4 should be ignored.

This initial presentation of a 3D computer graphic (Figure 3) and a 2D-contour map (Figure 4) shows the former to be a qualitatively pleasing overview showing roughly areas possible and impossible for kinetic pathways. However, for quantitative readings of $[\xi_1,\xi_2]$, the location of the kinetic boundaries and definitive assurance that the pathway is indeed yielding a decrease in the Gibbs energy, the 2D contour map is more useful. In the examples to follow, only 2D contour maps will be presented to save space; the reader is referred to Vuddagiri[23] for the corresponding 3D computer graphic. Alternately, readers can use eqs 20, 23, and 24 to provide their own 3D graphics.

Effect of Initial Conditions. The initial conditions affect the Gibbs surface including the global equilibrium. In particular, they change the kinetic boundaries and thus the optimum yields of a particular product, assuming that catalysts can be found to steer the reaction pathway. Here we start with the case above, Figures 3 and 4, as the Series Case and then change only the starting conditions as summarized in Figure 5. The other three variations are (a) the Parallel Case

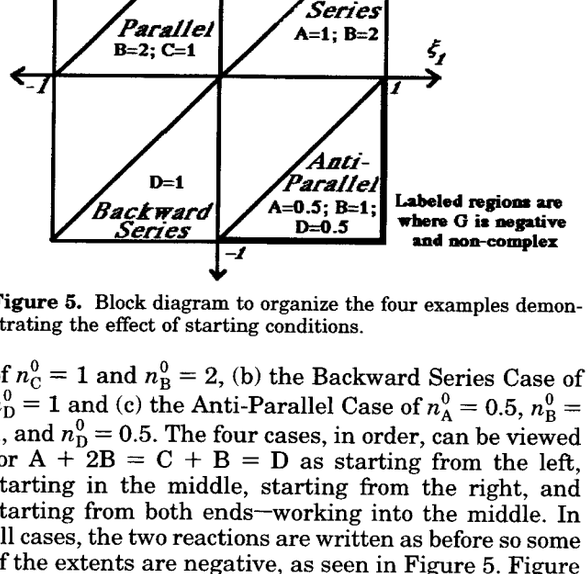

Figure 5. Block diagram to organize the four examples demonstrating the effect of starting conditions.

of $n_C^0 = 1$ and $n_B^0 = 2$, (b) the Backward Series Case of $n_D^0 = 1$ and (c) the Anti-Parallel Case of $n_A^0 = 0.5$, $n_B^0 = 1$, and $n_D^0 = 0.5$. The four cases, in order, can be viewed for A + 2B = C + B = D as starting from the left, starting in the middle, starting from the right, and starting from both ends—working into the middle. In all cases, the two reactions are written as before so some of the extents are negative, as seen in Figure 5. Figure 6 illustrates this point for the Parallel Case where the starting point is at the origin. When the reaction rates are $\mathcal{RS}$, we jump from the origin to near [−0.4, 0] and then along the curve marked F to the global equilibrium. On the other hand, when the rates are $\mathcal{SF}$, we jump

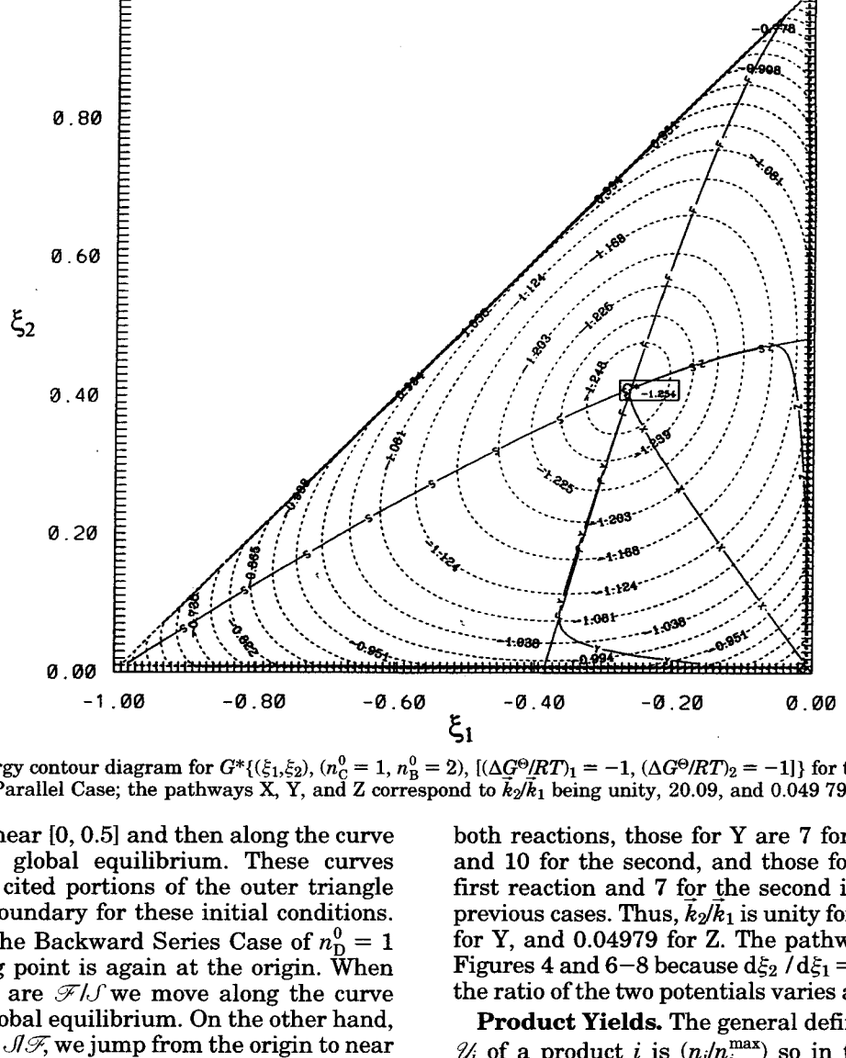

Figure 6. Gibbs energy contour diagram for $G^*\{(\xi_1,\xi_2), (n_C^0 = 1, n_B^0 = 2), [(\Delta G^\ominus/RT)_1 = -1, (\Delta G^\ominus/RT)_2 = -1]\}$ for the reaction A + 2B = 1 = B + C = 2 = D; Parallel Case; the pathways X, Y, and Z correspond to $\vec{k}_2/\vec{k}_1$ being unity, 20.09, and 0.049 79, respectively.

from the origin to near [0, 0.5] and then along the curve marked S to the global equilibrium. These curves together with the cited portions of the outer triangle form the kinetic boundary for these initial conditions.

Figure 7 is for the Backward Series Case of $n_D^0 = 1$ where the starting point is again at the origin. When the reaction rates are $\mathcal{F}/\mathcal{S}$ we move along the curve marked F to the global equilibrium. On the other hand, when the rates are $\mathcal{S}/\mathcal{F}$, we jump from the origin to near [0, −0.53] and then along the curve marked S to the global equilibrium. These curves together with the cited portion of the vertical axis form the kinetic boundary for these initial conditions.

Figure 8 is for the Anti-Parallel Case of $n_A^0 = 0.5$, $n_B^0 = 1$, and $n_D^0 = 0.5$, where the starting point is again at the origin. When the reaction rates are $\mathcal{F}/\mathcal{S}$, we jump to near [0.26, 0] and then move along the curve marked F to the global equilibrium. On the other hand, when the rates are $\mathcal{S}/\mathcal{F}$, we jump from the origin to near [0, −0.20] and then along the curve marked S to the global equilibrium. These curves together with the cited portions of the two coordinate axes form the kinetic boundary for these initial conditions.

Other Pathways. Figures 4 and 6− 8 also show pathways marked X, Y, and Z, all lying, of course, within the kinetic boundary for each particular figure. These pathways were found using Arrenhius constants with eqs 18 and 19:

$$\vec{k}_2/\vec{k}_1 = \vec{k}_2^*/\vec{k}_1^* \exp[\vec{E}_{A,2}/RT - \vec{E}_{A,1}/RT] \qquad (26)$$

with the ratio of the preexponential Arrenhius constants, $\vec{k}_2^*/\vec{k}_1^*$, set to unity. The values of the forward Arrenhius constants $\vec{E}_{A,j}/RT$ for pathway X are 10 for both reactions, those for Y are 7 for the first reaction and 10 for the second, and those for Z are 10 for the first reaction and 7 for the second in each of the four previous cases. Thus, $\vec{k}_2/\vec{k}_1$ is unity for pathway X, 20.09 for Y, and 0.04979 for Z. The pathways are curved in Figures 4 and 6−8 because $d\xi_2/d\xi_1 = (\vec{k}_2/\vec{k}_1)(\mathcal{P}_2/\mathcal{P}_1)$ and the ratio of the two potentials varies along the pathway.

Product Yields. The general definition for the yield $\mathcal{Y}_i$ of a product i is (n_i/n_i^{max}) so in the four examples above we can examine how the yield of a particular product changes along a reaction pathway. In the Series Case, the yield of C is $\mathcal{Y}_C = \xi_1 - \xi_2$; from Figure 4 and previous values, $\mathcal{Y}_C$ is 0.34 (34%) at equilibrium, but in the $\mathcal{F}/\mathcal{S}$ case marked F where $[\xi_1,\xi_2]$ and jumps to [0.61, 0] the value of $\mathcal{Y}_C$ is 0.61. Thus, $\mathcal{Y}_C$ goes through a maximum on the $(\mathcal{F}/\mathcal{S}$ and also the Y pathway of Figure 4. It rises on the X pathway to be about 0.3 when $\xi_1 = \sim 0.4$ and remains roughly constant onto equilibrium. It is monotonically increasing along the Z and $\mathcal{S}/\mathcal{F}$ paths. On the other hand, the yield of D is $\mathcal{Y}_D = \xi_2$; in the Series Case, $(\mathcal{F}/\mathcal{S})$, we jump to near [0.26, 0] and then move along the curve marked F to the global equilibrium, along all possible reaction paths.

In the Parallel Case of Figure 6, $\mathcal{Y}_D = \xi_2$ and $\mathcal{Y}_A = -\xi_1$. The $\mathcal{F}/\mathcal{S}$ path marked F shows a jump from the origin to near [−0.4, 0] and then to equilibrium at [−0.26, 0.42] so $\mathcal{Y}_D$ increases monotonically but $\mathcal{Y}_A$ is maximum at [−0.4, 0]. Conversely, for the $\mathcal{S}/\mathcal{F}$ path marked S, there is initially a jump to near [0, 0.5] and then to the equilibrium so $\mathcal{Y}_D$ is maximum at [0, 0.5] whereas $\mathcal{Y}_A$ increases monotonically. For the Backward Series Case of Figure 7, $\mathcal{Y}_C = \xi_1 - \xi_2$, $\mathcal{Y}_B = -(\xi_1 + \xi_2)/2$, and $\mathcal{Y}_A = -\xi_1$. For the $\mathcal{S}/\mathcal{F}$ path marked S, there is initially a jump to near [0, −0.53] and then to the

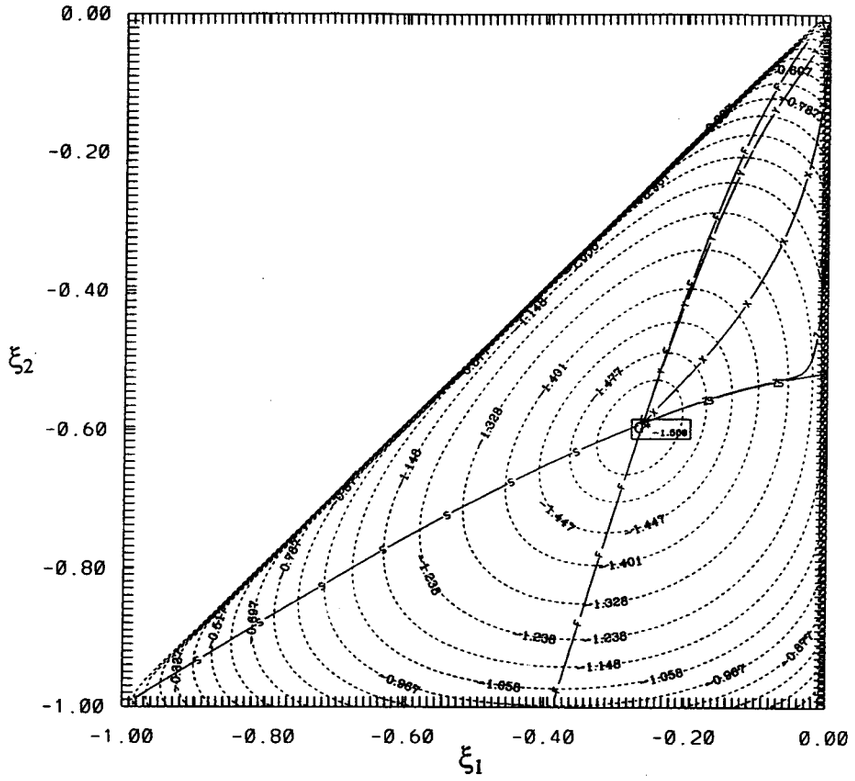

Figure 7. Gibbs energy contour diagram for $G^*\{(\xi_1,\xi_2), (n_D^0 = 1), [(\Delta G^\ominus/RT)_1 = -1, (\Delta G^\ominus/RT)_2 = -1]\}$ for the reaction A + 2B = 1 = B + C = 2 = D; Backward Series Case; the pathways X, Y, and Z correspond to $\bar{k}_2/\bar{k}_1$ being unity, 20.09, and 0.049 79, respectively.

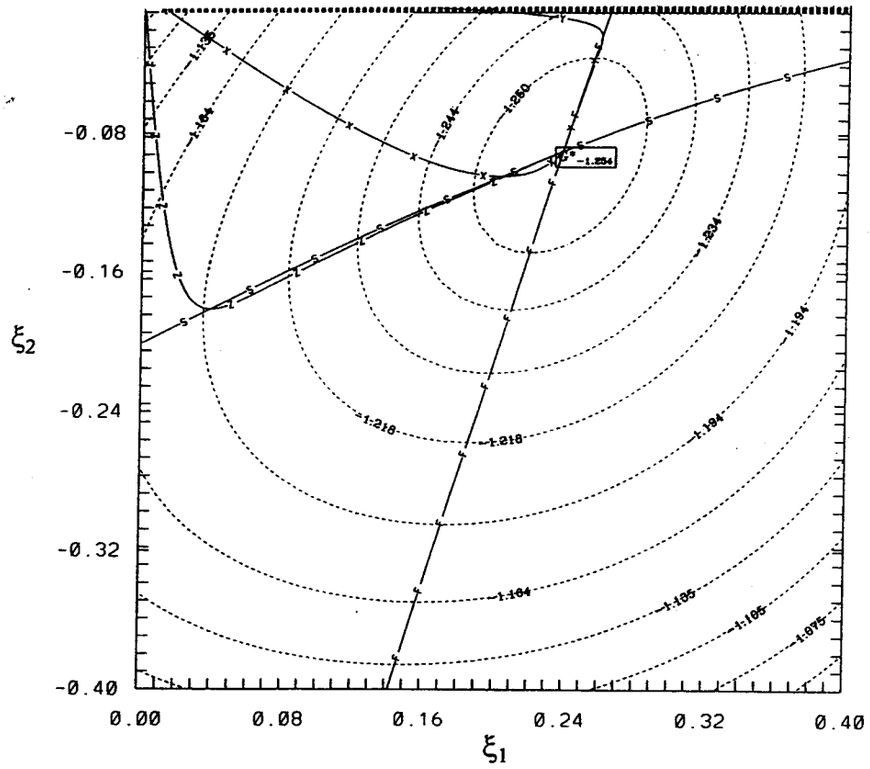

Figure 8. Gibbs energy contour diagram for $G^*\{(\xi_1,\xi_2), (n_A^0 = 0.5, n_B^0 = 1, n_D^0 = 0.5), [(\Delta G^\ominus/RT)_1 = -1, (\Delta G^\ominus/RT)_2 = -1]\}$ for the reaction A + 2B = 1 = B + C = 2 = D; Anti-Parallel Case; the pathways X, Y, and Z correspond to $\bar{k}_2/\bar{k}_1$ being unity, 20.09, and 0.049 79, respectively.

equilibrium near [−0.27, −0.60], causing $\mathcal{Y}_C$ to maximize at [0, −0.53] whereas $\mathcal{Y}_B$ and $\mathcal{Y}_A$ are monotonically increasing. For the Anti-Parallel Case of Figure 8, $\mathcal{Y}_C = \xi_1 - \xi_2$ and the equilibrium is at [0.24, −0.9] where

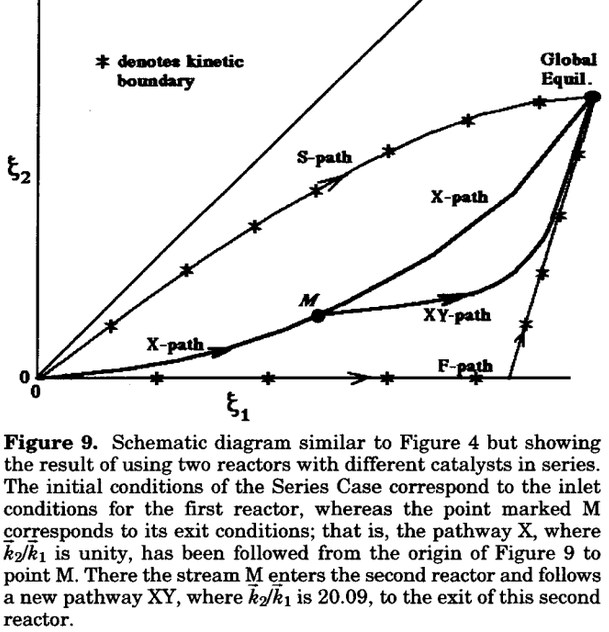

Figure 9. Schematic diagram similar to Figure 4 but showing the result of using two reactors with different catalysts in series. The initial conditions of the Series Case correspond to the inlet conditions for the first reactor, whereas the point marked M corresponds to its exit conditions; that is, the pathway X, where $\vec{k}_2/\vec{k}_1$ is unity, has been followed from the origin of Figure 9 to point M. There the stream M enters the second reactor and follows a new pathway XY, where $\vec{k}_2/\vec{k}_1$ is 20.09, to the exit of this second reactor.

$\mathcal{Y}_C = 0.33$. For $\mathcal{F}/\mathcal{S}$ we jump to near [0.26, 0] and then move along the curve marked F to the global equilibrium; $\mathcal{Y}_C$ increases monotonically along this pathway as well as along the $\mathcal{F}/\mathcal{S}$ path marked F and also other possible pathways.

Three Reactions in Series and Y Formation. We briefly summarize the recent work of Vuddagiri[23] for the reactions (1) A + 2B = C + B = D = E and (2) A + B = C → C + B = D or → C = E.

For starting conditions of $n_A^0 = 1$ and $n_B^0 = 2$ and with all $\Delta G_j^0/RT = -1$, 2D contour maps are examined for the first case when, in turn, one of the reactions is instantaneous. For the second case of the Y formation, one must examine the second and third reactions, which are in parallel, to see which is rate determining. Y formations can be considered as a combination of series and parallel reactions. Vuddagiri[23] has also examined the case where the second reaction (to form D) is instantaneous.

Discussion

In practice, flow reactors use various catalysts, but seldom does the exit stream reach equilibrium. By using a variety of compositions in the inlet stream (i.e., initial conditions), it has been shown that the kinetic boundaries can be greatly changed and that the yield of a particular product may or may not be maximized on a particular pathway (i.e., with a particular set of catalysts). However, the flow reactors can themselves be placed in different configurations (e.g., series, parallel, Y, or delta) with different catalysts in each reactor so that the pathways can be creatively altered to maximize profits. Here, we provide a few simple examples using the 2D contour map developed above.

First, two reactors with different catalysts are placed in series. One can deduce from Figure 4, for example, what would happen if we start on the pathway marked X for the first reactor, where $\vec{k}_2/\vec{k}_1$ is unity, and proceed to a point M in Figure 9 where the flow stream exits the first reactor and enters the second reactor where it follows a pathway XY where $\vec{k}_2/\vec{k}_1$ is 20.09, the same as for path Y. We have added flexibility to our pathways, but we still cannot go outside the kinetic boundaries set by our initial conditions and the Gibbs surface for this simple example.

Second, we can place two reactors in parallel with different starting conditions for each. Then we can mix the exit streams from the two reactors before entering a third reactor. Mixing is one way to *jump over* a kinetic boundary to get into a region where a particular product yield may be well above equilibrium.

When the reaction system is not a single phase, the present methods can be applied to liquid solutions and to multiphase, multireaction cases. For example, for dilute liquid solutions (e.g., aqueous) an equation for G^* results where $\mu_i^\ominus$, the chemical potential of i in its general standard state [perfect gas, liquid, solid, or aqueous], generally does come from multiplicity of standard states; y_i is replaced by $\lambda_i x_i$, where x_i is the liquid-phase mole fraction and λ_i is a dimensionless constant such as $\mathcal{H}_{is}/P_i^\ominus$), where $\mathcal{H}_{is}$ is Henry's constant for solute i in the solvent (water) and $P_i^\ominus$ is the standard state pressure (1 bar for perfect gas but usually the vapor pressure for pure liquid or solid standard states). For strong, nonideal liquid solutions, λ_i is replaced by the activity coefficient γ_i.

When the reaction conditions are not isobaric/isothermal, we have performed a limited number of calculations. No additional problems were encountered except it is more difficult to visualize the 3D G^* diagrams—sometimes it helps to think of a series of isobaric/isothermal diagrams with the G^* surface shifting with changing T or P or both. Some specific cases are as follows:

A. Isochoric/Isothermal: Minimize the Helmholtz energy instead of Gibbs. It is especially easy to calculate with an equation-of-state (EoS) simulator.

B. Isochoric/Adiabatic: Here the internal energy would be constant except for the heats of reaction. Use an energy balance and graph entropy (maximized) instead of the Gibbs energy. Note the many safety applications including runaway reactions which are typically strongly exothermic.

Conclusions

The combined kinetics and irreversible thermodynamics of multiple reactions can be traced by computer graphic techniques to understand how to optimize selectivities and sometimes produce higher yields of a particular product than what occurs at equilibrium. Some call this *cheating thermodynamics* but, of course, it is not—indeed, understanding the thermodynamics and kinetics together with *educated planning and testing* leads to much higher probabilities of success in terms of maximization of yields and thus profits than random luck.

1. So-called kinetic boundaries cannot be crossed without negative reaction rate constants. However, often one may, nevertheless, obtain yields higher than those at equilibrium by skillful navigation within these boundaries.

2. While the present examples were for simple reaction networks, more complex networks are amenable to these procedures as long as there are only a few rate-controlling reactions. Very fast reactions have their instantaneous $\Delta G = 0$, at all times, and so they *follow*

along with what is happening to the rate-controlling reactions. Either very slow reactions can be rate controlling or they may be in parallel with faster reactions—meaning they can be ignored. A careful analysis of the electrical diagram is required initially for complex chemical networks.

3. The present examples can also be extended to cases, which do not assume perfect gas mixtures, including multiple-phase reactions, and to reaction processes that are not isothermal/isobaric.

Acknowledgment

Many of the problems addressed here were outlined, in the context of biological reactions, to the corresponding author by Prof. J. C. Liao in Nov of 1990. Early input from Prof. J. C. Slattery is also acknowledged. We also thank the National Science Foundation (Grant 9317812) and the Texas Engineering Experiment Station for partial support of this effort.

Nomenclature

$\mathcal{A}_j$ = affinity of reaction j, J/mol
a_i = activity of component i
C = capacitance, F
E_A = activation energy, J/mol
F = pathway where the first reaction is fast and the second slow
f_i = fugacity of component i, bar
G = Gibbs energy, J/mol
G^* = dimensionless Gibbs energy parameter with the same minimization properties as G_T
$\mathcal{H}_{is}$ = Henry's constant for solute i in the solvent
k_j = kinetic rate constant for reaction j, mol/s
$K = \prod_i a^{\nu_i}$
K_e = equilibrium constant
n_i = moles of component i
$\mathcal{N}$ = number of chemical species including compounds, radicals, and intermediates
$\mathcal{P}_j$ = potential function of reaction j
P = total pressure, bar
p_i = partial pressure of component i or Py_i
r_j = net rate of the jth reaction, mol/s
R = gas constant, 8.314 J/(mol K)
$\mathcal{R}$ = total number of independent reactions
$\mathcal{S}$ = pathway where the first reaction is slow and the second reaction fast
S = entropy, J/(mol K)
T = temperature, K
t = time, s
X, Y, Z = pathways defined in text
$\mathcal{Y}_i$ = yield of component i
y_i = mole fraction of component i

Greek Symbols

α_i = order of the net reaction for component i
Δ = change in a property
χ = stoichiometric number
ν_j = net stoichiometric coefficient for reaction j
ν_{ij} = stoichiometric coefficient of component i for reaction j
ξ_j = extent of reaction j, mol
μ_i = chemical potential of component i

Subscripts

e = equilibrium
i = component counter
j = reaction counter
T = total quantity

Superscripts

Θ = standard state [gas, liquid, solid, or aqueous]
0 = initial quantity
$\rightarrow$ = forward reaction
$\leftarrow$ = reverse reaction
$\hat{}$ = mixture property
$\bar{}$ = averaged value

Literature Cited

(1) Denbigh, K. G. *Chemical Reactor Theory*; Cambridge University Press: Cambridge, 1965; p 25.
(2) Eu, B. C. *Kinetic Theory and Irreversible Thermodynamics*; John Wiley & Sons: New York, 1992.
(3) Hollingsworth, C. A. Kinetics and Equilibria of Complex Reactions. *J. Chem. Phys.* **1957**, *27* (6), 1346.
(4) Horiuti, J. Significance and Experimental Determination of Stoichiometric Number. *J. Catal.* **1962**, *1*, 199.
(5) Blum, E. H.; Luus, R. Thermodynamic Consistency of Reaction Rate Expression. *Chem. Eng. Sci.* **1964**, *19*, 322.
(6) Van Rysselberghe, P. Consistency Between Kinetics and Thermodynamics. *Chem. Eng. Sci.* **1967**, *22*, 706.
(7) Boudart, M. Consistency Between Kinetics and Thermodynamics. *J. Phys. Chem.* **1976**, *80* (26), 2869.
(8) de Donder, Th. *L'Affinitè*; Gauthiers-Villars: Paris, 1927.
(9) Prigogine, I.; Outer, P.; Herbo, C. L. Affinity and Reaction Rate Close to Equilibrium. *J. Phys. Colloid Chem.* **1948**, *52*, 321.
(10) Manes, M.; Hofer, L. J. E.; Weller, S. Classical Thermodyanmics and Reaction Rates Close to Equilibrium. *J. Chem. Phys.* **1950**, *18* (10), 1355.
(11) Gilkerson, W. R.; Jones, M. M.; Gallup, G. A. Chemical Reactions Near Equilibrium. *J. Chem. Phys.* **1952**, *20* (7), 1182.
(12) Hollingsworth, C. A. Equilibrium and the Rate Laws for Forward and Reverse Reactions. *J. Chem. Phys.* **1952**, *20* (5), 921.
(13) Zwolinski, B. J.; Marcus, R. J. Rates of Chemical Reactions Near Equilibrium. *J. Chem. Phys.* **1954**, *22* (9), 2235.
(14) Van Rysselberghe, P. Reaction Velocity Near Equilibrium. *J. Chem. Phys.* **1954**, *22* (4), 761.
(15) Kondepudi, D.; Prigogine, I. *Modern Thermodynamics*; John Wiley & Sons: New York, 1998.
(16) Temkin, M. I. *Dokl. Akad. Nauk SSSR* **1963**, *152*, 156.
(17) Happel, J. Study of Kinetic Structure Using Marked Atoms. *Catal. Rev.* **1972**, *6*, 221.
(18) Temkin, O. N.; Zeigarnik, A. V.; Bonchev, D. *Chemical Reaction Networks*; CRC Press: New York, 1996.
(19) Wei, J.; Prater, C. D. The Structure and Analysis of Complex Chemical Reaction Systems. In *Advances in Catalysis*; Eley, D. D., Selwood, P. W., Weisz, P. B., Eds.; Academic Press: New York, 1962; Vol. 13, pp 203–392.
(20) Wei, J.; Prater, C. D. A New Approach to First-Order Chemical Reaction Systems. *AIChE J.* **1963**, *9*, 77.
(21) Missen, R. W.; Mims, C. A.; Saville, B. A. *Introduction to Chemical Reaction Engineering and Kinetics*; John Wiley & Sons: New York, 1999; p 106.
(22) Smith, J. M.; Van Ness, H. C.; Abbott, M. M. *Introduction to Chemical Engineering Thermodynamics*, 5th ed.; McGraw-Hill: New York, 1996.
(23) Vuddagiri, S. R. The Effect of Equilibrium/Non-Equilibrium Thermodynamics on Rate Processes. Ph.D. Dissertation, Texas A&M University, College Station, TX, 1998.

Received for review June 9, 1999
Revised manuscript received October 21, 1999
Accepted November 15, 1999

IE9904091